

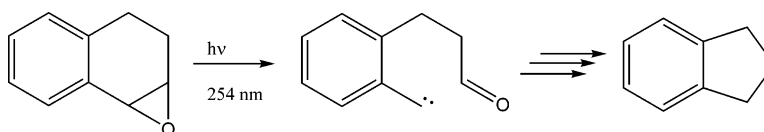
## Photochemistry of 1,2-Dihydronaphthalene Oxide: Concurrent Triplet and Singlet Processes via Singlet Excitation

Rick C. White,\* Benny E. Arney Jr.,\* and Katherine M. White

Department of Chemistry, Box 2117, Sam Houston State University, Huntsville, Texas 77341

chm\_bea@shsu.edu; chm\_rcw@shsu.edu

Received July 7, 2006



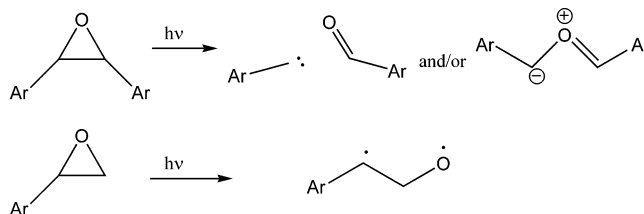
The photochemistry of 1,2-dihydronaphthalene oxide (254 nm) was reexamined and indan was found to be a primary photoproduct, as well as the traditionally assumed secondary photoproduct. Quenching studies demonstrated that indan, as a primary photoproduct, is derived from a triplet pathway, competing with a singlet route, back to the ground state surface. CASSCF calculations strongly suggest that the triplet pathway consists of a dissociation of the oxirane moiety to give a triplet carbene and aldehyde, which via hydrogen abstraction–decarbonylation–ISC recloses to give indan. Conical intersections corresponding to the presumed 1,2-hydrogen shift and 1,2-alkyl shift to give 2-tetralone and 1-indan-carbaldehyde, respectively, were located computationally.

### Introduction

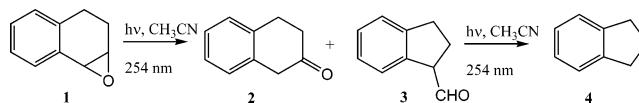
Early work on the photochemistry of aryloxiranes led to the adoption of two distinct major photochemical mechanisms for these systems. In the first, vicinal diaryloxiranes underwent photochemical scission of the benzylic carbon–carbon bond of the oxirane unit to produce carbenes<sup>1</sup> or carbonyl ylids<sup>2</sup> which were characterized by trapping experiments with alcohols<sup>1a</sup> and with double bonds.<sup>1b,3</sup> In the second, monoaryloxiranes underwent carbon–oxygen bond cleavage to generate 1,3-diradicals<sup>4</sup> (Scheme 1). In general, it has been accepted that each aryloxirane only follows one path or the other depending on structure.

It has been reported that photolysis of 1,2-dihydronaphthalene oxide<sup>5</sup> (**1**) yielded  $\beta$ -tetralone (**2**) and indan-1-carbaldehyde (**3**)

### SCHEME 1. Accepted Photochemical Pathways for Aryloxiranes



### SCHEME 2. Hitherto Accepted Product Formation Sequence for the Photolysis of 1,2-Dihydronaphthalene Oxide



as the primary photoproducts (Scheme 2). The assumed pathway for this reaction has been the initial homolysis of the benzylic oxirane C–O bond giving the corresponding 1,3-diradical which subsequently underwent 1,2-hydrogen migration or 1,2-alkyl migration to form **2** or **3**, respectively. Indan (**4**) was also formed early in the photolysis and was presumed to arise as a secondary photoproduct from the photoinduced decarbonylation of **3**, but its reported rate of formation far exceeded what would be

\* To whom correspondence should be addressed. Tel: 1-936-294-1531. Fax: 1-936-294-4996. E-mail: chm\_bea@shsu.edu.

(1) (a) Griffin, G. W.; Smith, R. L.; Manmade, A. *J. Org. Chem.* **1976**, *41*, 338. (b) Smith, R. L.; Manmade, A.; Griffin, G. W. *J. Heterocycl. Chem.* **1969**, *6*, 443. (c) Trozzolo, A. M.; Yager, W. A.; Griffin, G. W.; Kristinnson, H.; Sarkar, I. *J. Am. Chem. Soc.* **1967**, *89*, 3357.

(2) (a) Becker, R. S.; Bost, R.; Bertioniere, N. R.; Smoth, R. L.; Griffin, G. W. *J. Am. Chem. Soc.* **1970**, *92*, 1302. (b) Do-Minh, T.; Trozzolo, A. M.; Griffin, G. W. *J. Am. Chem. Soc.* **1970**, *92*, 1402. (c) Griffin, G. W.; Ishikawa, K.; Lev, I. J. *J. Am. Chem. Soc.* **1976**, *98*, 5697.

(3) (a) Brokatzky-Geiger, J.; Eberbach, W. *Tetrahedron Lett.* **1984**, *25*, 1137. (b) Kristinnson, H.; Griffin, G. W. *Angew. Chem., Int. Ed. Engl.* **1965**, *4*, 868.

(4) Arney, B. E., Jr.; White, R. C.; Ramanathan, A.; Barham, L.; Sherrod, S.; McCall, P.; Livanec, P.; Mangus, K.; White, K. *Photochem. Photobiol. Sci.* **2004**, *3*, 851 and references contained therein.

(5) Padwa, A.; Griffin, G. W. In *Organic Photochemistry*; Marcel Dekker Inc.: New York, 1976; Vol. 3, pp 41–121.

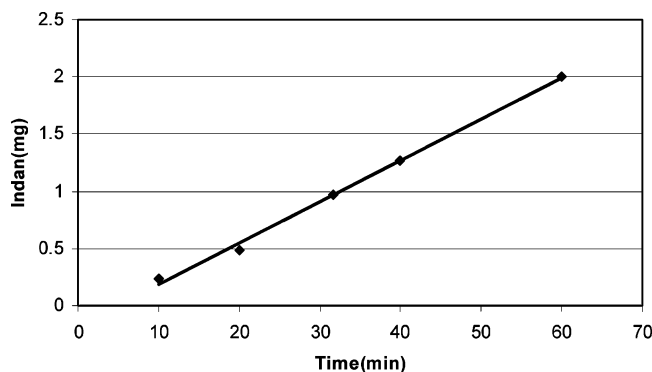


**FIGURE 1.** Indan formation (mg) versus time (min) (0.06 M in CH<sub>3</sub>-CN, 254 nm).

consistent with this model.<sup>6</sup> Curiously, *cis*-1,2-dihydroxy-1,2,3,4-tetrahydronaphthalene carbonate<sup>7</sup> yielded only **1**, **2**, and **3** under photolysis with no reported observation of the early formation of **4** despite presumably proceeding via the same 1,3-diradical.

Previously, we reported on the anomalously high yield of indan (**4**)<sup>6</sup> early in the irradiation of **1** (245 nm) requiring us to reexamine the presumption of **4** being solely a secondary photoproduct. Measurement of the quantum yield for indan formation from **1** ( $\Phi = 0.51$ ) showed it to be several times greater than its quantum yield from **2** ( $\Phi = 0.10$ ).<sup>6</sup> The possibility of a photoinduced bimolecular radical process acting on **1** was examined as a possible cause but was not supported by experiment.<sup>6</sup> Sensitization of the photolysis of **3** to **4** by the more abundant starting epoxide, **1**, was also examined and found to be probable but could not account for the production of **4** in excess<sup>6</sup> of the production of **3**. This behavior reasonably precluded **3** from being the dominant/sole photochemical precursor to **4** and strongly suggested the existence of an additional photochemical pathway to **4** from **1**. Notably this type of behavior has also been reported in the photolysis of styrene oxide to give bibenzyl (as a secondary photoproduct), where bibenzyl formation was observed to be much faster from styrene oxide than from its presumed immediate precursor phenylacetaldehyde.<sup>8</sup> These inconsistencies have prompted us to investigate the formation of **4** in the photolysis of **1**. Our experimental and computational findings are reported herein and compared with the accepted model for the photochemistry of **1**.

## Results and Discussion

**Photolysis Studies:** Examination of the formation of **4** (mg) versus time, using short time intervals of 0–60 min, displayed linear growth ( $R^2 = 0.9971$ ), showing it to be a primary photoproduct in the photolysis of **1**. No upward curvature, expected of a biphotonic product, was noted until after a significant time interval such that the concentration of **3** was significant (Figure 1).

Although **1** failed to react under triplet sensitized photolysis<sup>6</sup> (no observable **2**, **3**, or **4**), early formation of **4** was completely quenched when direct irradiation was carried out in the presence of isoprene, while the rates of formation of **2** and **3** were

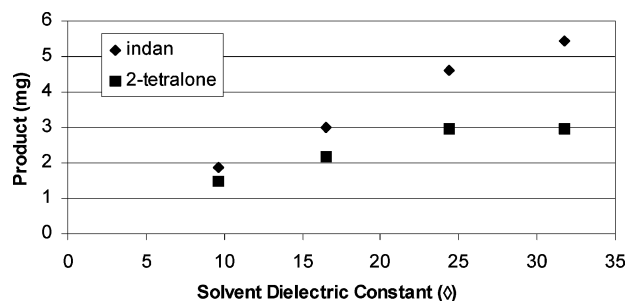


**FIGURE 2.** Yield of **2** and **4** versus solvent dielectric constant.

unaffected. Early primary formation of **4** must arise from a triplet pathway encountered after initial singlet excitation. Such pathways have been proposed for other unrelated systems.<sup>9</sup> A triplet–singlet surface crossing (ISC) near a low barrier to a ( $S_1/S_0$  or  $S_2/S_1$ ) conical intersection could provide a highly efficient conduit to populating the triplet surface near a molecular geometry inaccessible to an initially triplet sensitized ground state structure. Quenching of the triplet state could return the molecule to the ground state surface prior to significant changes in the molecular geometry along the pathway towards triplet photoproducts. In this case, we suppose that this would imply that the geometry would still resemble either the starting epoxide or the presumed 1,3-diradical that would return to **1** or continue along the singlet pathway, respectively.

In general, ground state radical reactions are not sensitive to solvent polarity; however, we have found that as the solvent polarity increased the ratio of indan to 2-tetralone also increased, as illustrated in the plot in Figure 2. Two implications were suggested by the plot. Enhanced indan formation, with increased polarity, indicated an increase in molecular or localized polarity in the early stages of indan formation. 2-Tetralone (**2**) formation also exhibited enhancement with solvent polarity but showed a limitation as its formation plateaus at higher dielectric constants. Extremely noteworthy in this regard is the virtually complete suppression of the formation of **2** when photolysis is carried out in protic solvents (MeOH, EtOH, or *t*-BuOH). This suppression is accompanied by an increase in the formation of aldehyde **3**. That **2** and **3** are probably derived from the same initially formed species (an excited state 1,3-diradical) is supported by this behavior, which suggests that the solvent can play a pivotal role in the evolution of the excited species on the excited state surface. In this instance, we suspect that extensive solvation involving the oxirane oxygen in the excited singlet ring-opened species effectively increases the potential barrier to the formation of **2** on the excited state surface or alternatively may decrease the barrier to form **3**.

Solutions consisted of 30 mg of **1** in solvents consisting of mixtures of hexane ( $\epsilon = 2.2$ ) and acetonitrile ( $\epsilon = 39.2$ ) in ratios (mL:mL) of 1:4, 2:3, 3:2, and 4:1, respectively. Dielectric constant of mixtures was calculated as the weighted average of the two solvents.

Finally, a subtle observation in the photolysis of **3** is the formation of indene, **5**, in addition to **4**.<sup>10</sup> In every photolysis of **3**, we noted that **5** was always produced in a small fraction (~5–10%) of the indan formation. We speculate that the deformylation of **3** proceeded via three paths (Scheme 3):

(6) White, R. C.; Wedyck, E. J.; Lynch, K. O. *J. Photochem. Photobiol. A: Chem.* **1993**, *71*, 127.

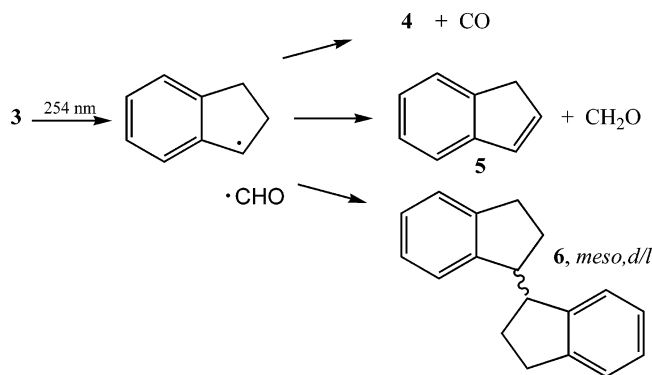
(7) White, R. C.; Drew, P.; Moorman, R. J. *Heterocycl. Chem.* **1988**, *25*, 1781.

(8) Kristinnson, H.; Griffin, G. W. *J. Am. Chem. Soc.* **1966**, *88*, 1579.

(9) Merchán, M.; Serrano-Andrés, L.; Robb, M. A.; Blancafort, L. *J. Am. Chem. Soc.* **2005**, *127*, 1820.

(10) White, R. C.; Arney, B. E. Unpublished results.

## SCHEME 3. Photoinduced Decarbonylation of 1-Indancarbaldehyde



hydrogen transfer from formyl to indanyl giving **4**,  $\alpha$ -hydrogen abstraction from indanyl by formyl giving **5** and formaldehyde, or biindanyl (**6**) formation<sup>11</sup> analogous to bibenzyl formation in the photolysis of phenylacetaldehyde.<sup>8</sup> However, **5** is never observed in the photolysis of **1** until very long reaction times are used, at which time traces of two components displaying the  $m/z$  of **6** also appear in the GC/MS trace. We have tentatively assigned these species to the DL- and *meso*-isomers of **6**.

**Computational Studies:** In light of the experimental results obtained, we chose to employ computational methods to examine possibilities for this system that are not directly observable experimentally. One of the more powerful computational methods for exploring photochemical reactions has been the use of MC-SCF computational techniques to locate and characterize molecular geometries of excited state species. Complete active space SCF (CASSCF) calculations provide configuration interaction of the ground state and excited state surfaces via utilization of a matrix of matrices, each one of which represents one of the possible electron excitation states or the ground state based on the selection of occupied and virtual orbitals with which to generate the possible states. Use of the CASSCF method also allows for the location of those molecular geometries where the ground state surface and the first excited state surface are degenerate, a point known as a conical intersection.<sup>12</sup> Conical intersections can serve as barrier-free, highly efficient passage points to the ground state surface where available relaxation modes determine the geometry changes probable along its pathway to a minima. CASSCF calculations<sup>13</sup> (CAS(4,4)/6-31G(d)) were performed (opt=conical algorithm) in our labs using the appropriate active spaces shown in Figure 3. Aromatic  $\pi$ -system orbitals were not included<sup>14</sup> in the utilized active spaces as accurate reaction energetics, excitation energies, and energy barriers were not within the scope of this work, which focused on the examination of potential photogenerated intermediates in the photolysis of the parent **3**. The aromatic  $\pi$ -system was viewed as a “photon antenna”<sup>15</sup> to gather light and supply the excitation to the oxirane moiety. Active space **I** included the two benzylic  $\sigma/\sigma^*$  orbital pairs of the epoxide moiety, which have been known to dissociate in some aryloxiranes under photolytic conditions. Active spaces **II** and **III** were modeled on the ubiquitously proposed singlet 1,3-diradical generally proposed as the primary intermediate in aryloxirane

(11) Formation of indanyl dimers is strongly suggested by the consistent presence of two high boiling components in the GC/MS analysis of the photolysis of **1**, both with base peaks of  $m/e = 145$  corresponding to indanyl.

(12) Robb, M. A.; Bernardi, F.; Olivucci, M. *Pure Appl. Chem.* **1995**, *67*, 783 and references contained therein.

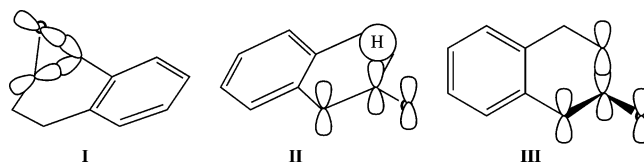


FIGURE 3. Active spaces utilized for CASSCF calculations.

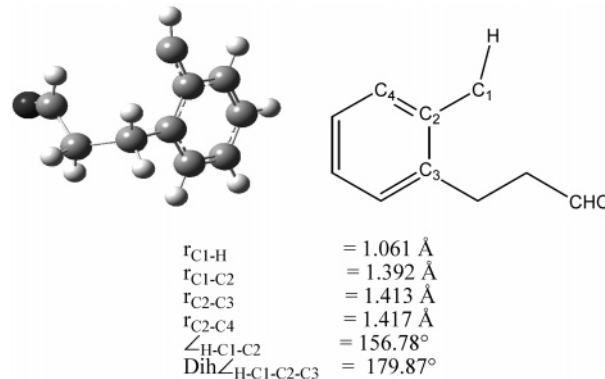


FIGURE 4. Views of conical intersection CCCI.

photochemistry, and they corresponded well with those commonly utilized in the location of hydrogen-allyl and alkyl-allyl-type conical intersections, respectively. All three active spaces (**I**, **II**, and **III**) successfully led to the location of conical intersections.

Active space **I** converged to a ( $S_1/S_0$ ) conical intersection (CCCI, Figure 4) with a geometry that corresponded to the complete dissociation of both benzylic  $\sigma$ -bonds of the aryloxirane ring, giving an aryl carbene and a formyl group as clearly depicted in the two views of CCCI. Additionally, a structurally similar ( $T_1/S_0$ ) surface crossing (TSC, Figure 5; also known as an intersystem crossing, ISC) was also located using an active space comprised of the two unshared valence orbitals of the carbenic carbon. Thus this carbenic-aldehyde structure is potentially accessible via a singlet or triplet pathway from the initial excited state structure. Triplet state arylcarbenes are well-known for hydrogen atom abstraction and if formed could readily abstract the aldehydic hydrogen<sup>16</sup> leading to decarbo-

(13) Frisch, M. J.; Trucks, G. W.; Schlegel, H. B.; Scuseria, G. E.; Robb, M. A.; Cheeseman, J. R.; Zakrzewski, V. G.; Montgomery, J. A., Jr.; Stratmann, R. E.; Burant, J. C.; Dapprich, S.; Millam, J. M.; Daniels, A. D.; Kudin, K. N.; Strain, M. C.; Farkas, O.; Tomasi, J.; Barone, V.; Cossi, M.; Cammi, R.; Mennucci, B.; Pomelli, C.; Adamo, C.; Clifford, S.; Ochterski, J.; Petersson, G. A.; Ayala, P. Y.; Cui, Q.; Morokuma, K.; Malick, D. K.; Rabuck, A. D.; Raghavachari, K.; Foresman, J. B.; Cioslowski, J.; Ortiz, J. V.; Stefanov, B. B.; Liu, G.; Liashenko, A.; Piskorz, P.; Komaromi, I.; Gomperts, R.; Martin, R. L.; Fox, D. J.; Keith, T.; Al-Laham, M. A.; Peng, C. Y.; Nanayakkara, A.; Gonzalez, C.; Challacombe, M.; Gill, P. M. W.; Johnson, B. G.; Chen, W.; Wong, M. W.; Andres, J. L.; Head-Gordon, M.; Replogle, E. S.; Pople, J. A. *Gaussian 98*, revision A.6; Gaussian, Inc.: Pittsburgh, PA, 1998.

(14) The requisite CASSCF(10,10)/6-31G(d) calculations on this system are beyond the capacity of our current computational facilities.

(15) Celani, P.; Bernardi, F.; Olivucci, M.; Robb, M. A. *J. Am. Chem. Soc.* **1997**, *119*, 10815.

(16) (a) A similar ring formation from a triplet carbene can be seen in: Tomioka, H.; Okada, H.; Watanabe, T.; Banno, K.; Komatsu, K.; Hirai, K. *J. Am. Chem. Soc.* **1997**, *119*, 1582. (b) Aldehydic hydrogen dissociation energy (~86.0 kcal/mol) is comparable to that of a benzylic hydrogen (88.0 kcal/mol): McMillen, D. F.; Golden, D. M. *Annu. Rev. Phys. Chem.* **1982**, *33*, 493.

(17) (a) Wilsey, S.; Houk, K. N. *J. Am. Chem. Soc.* **2000**, *122*, 2651. (b) Wilsey, S.; Houk, K. N. *J. Am. Chem. Soc.* **2002**, *124*, 11182.

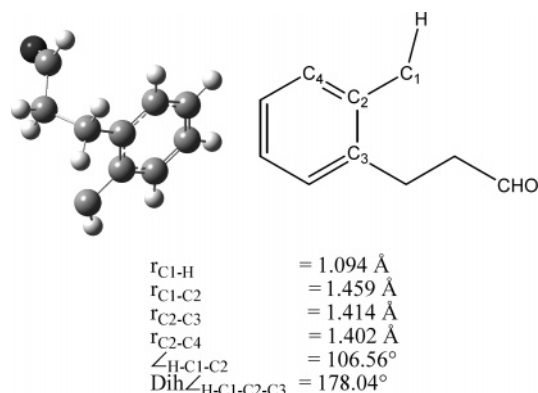
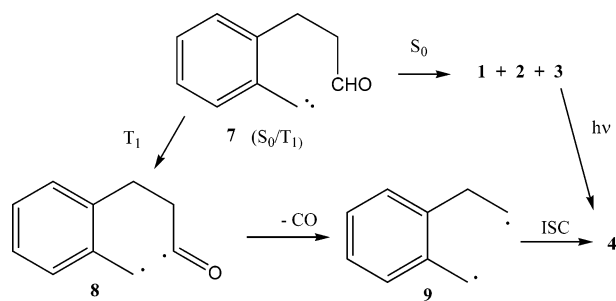


FIGURE 5. Views of conical intersection TSC.

#### SCHEME 4. Carbenic Pathway to Indan Formation



nylation followed by intersystem crossing (ISC) and ring closure to give indan **4** (Scheme 4). We speculate that, being intramolecular, these processes would proceed rapidly and relatively unimpeded providing a pathway to the formation of **4** that is independent of the formation of **3**.

Examination of the energetics of the triplet mechanism outlined in Scheme 4 was performed computationally at the UB3LYP/6-311G(d) level (Figure 6). The transition state (**TS1**) for the abstraction of the aldehydic hydrogen by the triplet carbene lies only  $\sim 4.5$  kcal/mol above **7**, strongly supporting a facile path to **8** which is  $\sim 22.1$  kcal/mol lower in energy than **7**. If these results are representative, then the path from **7** to **8** is virtually irreversible due to the difference in barriers to **TS1** (4.5 vs 26.6 kcal/mol). Transition state (**TS2**), for the decarbonylation of **8**, is much more accessible than **TS1**,  $\sim 15.9$  versus 26.6 kcal/mol, providing an efficient avenue to diradical **9**, which on intersystem crossing will close to give **4**. Single-point singlet energy calculation for the geometry obtained optimizing triplet **9&CO** gives an energy that differs by less than 0.05 kcal/mol, suggesting a highly efficient ISC then ring closure.

The conical intersection located using active space **II** was a hydrogen–allyl-type<sup>17</sup> conical (HACI, Figure 7) intersection that displayed extreme lengthening of the C1–H1 bond ( $r_{\text{C-H}} = 1.732 \text{ \AA}$ ) and lateral displacement toward the oxygen ( $r_{\text{O-H}} = 1.756 \text{ \AA}$ ) consistent with examples from previously calculated hydrogen–allyl-type conical intersections.<sup>17</sup> However, the position of the hydrogen in HACI was virtually centered over the C–O bond with the benzylic center apparently interacting with the aromatic  $\pi$ -system and not with the hydrogen. The asymmetry of the position of the hydrogen in HACI is rational due to the greater contribution of oxygen to the bonding MO's. The predicted shortening of the O–C1, C1–C2, and C2–C3  $\sigma$ -bonds denotes extensive  $\pi$ -interaction with indications of a developing double bond between C1 and C2. Normal mode analysis of the geometry at HACI indicates that it is a second-

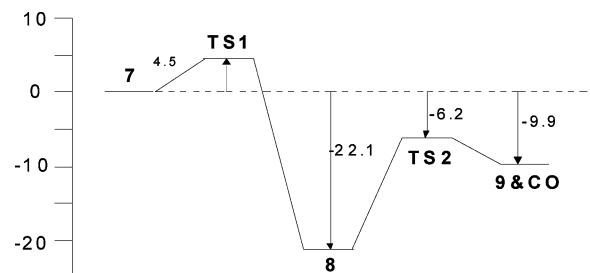


FIGURE 6. Energy profile for the triplet carbene–aldehyde hydrogen abstraction mechanism. Calculations were performed at the UB3LYP/6-311G(d) level. **TS1** is the transition state for H transfer; **TS2** is the transition state for decarbonylation of **8**, and **9&CO** stands for **9** and CO. Energy for **9&CO** was obtained by optimizing the dissociation from **TS2**.

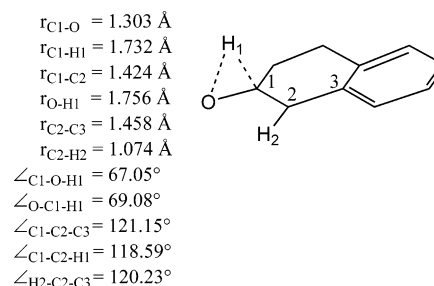


FIGURE 7. Conical intersection HACI.

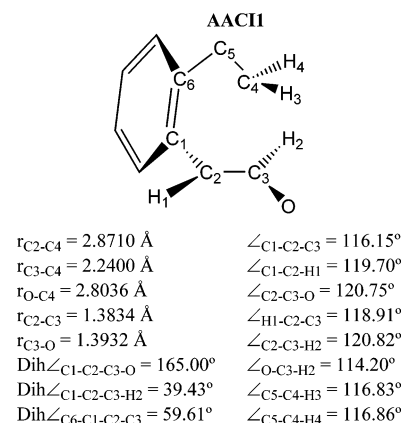


FIGURE 8. Structure of conical intersection AACII.

order saddle-point by two imaginary frequencies corresponding to homolytic dissociation of the hydrogen and migration of the hydrogen between O and C1. Geometrically, this conical intersection appears as a functional equivalent for a transition state for the ubiquitous 1,2-hydrogen migration observed in the chemistry of 1,3-diradicals and is consistent with the observed regiochemistry for such migrations. As such, if it arises from the supposed ring-opened 1,3-diradical, then the ring opening leads to the 1,3-diradical as a species on an excited state surface (probably  $S_1$ ) with conical intersection HACI providing a path to the ground state surface.

Two distinct conical intersections, corresponding to active space **III**, were located and both were clearly alkyl–allyl-type<sup>17</sup> conical intersections (AACII and AACI2, Figures 8 and 9, respectively) displaying lengthening of the C3–C4 bonds ( $r_{\text{C2-C3}} = 2.24$  and  $2.23 \text{ \AA}$ , respectively) consistent with reported values. Normal mode analysis performed on the geometries, AACII and AACI2, showed both to be second-order saddle-

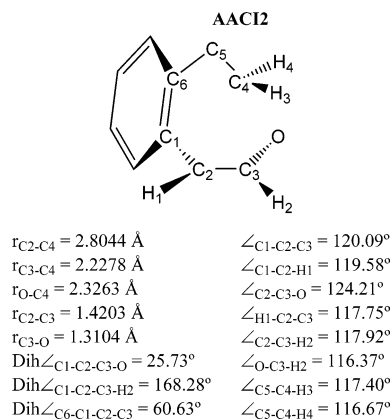


FIGURE 9. Structure of conical intersection AACI2.

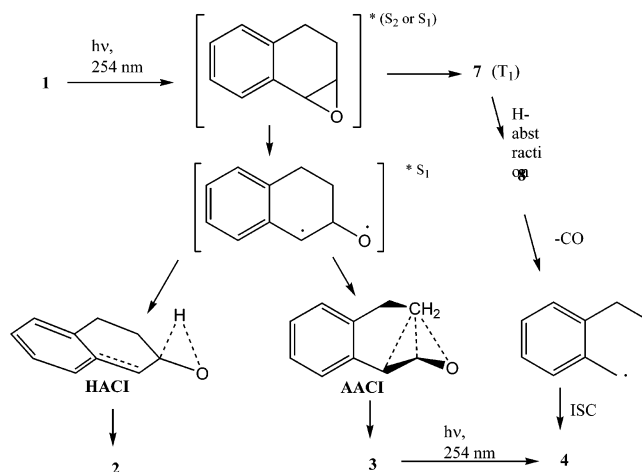
points. The two imaginary modes correspond to homolytic dissociation of the C3–C4 bond and to migration of C4 between C2–C3 for both AACI1 and AACI2. Geometrically, these CI's provide an efficient pathway to the formation of aldehyde **3**. Since aldehyde **3** is never formed in more than small amounts and is apparently a minor reaction pathway, we would speculate that there exists a barrier to accessing these pathways, at least relative to the others.

### Conclusion

The classic view of the aryl oxirane photochemistry has characterized these systems as an exclusive dichotomy, following either a dissociative path, as in the case of the diaryloxiranes, or a path of ring-opening cleavage of the benzylic C–O bond, as accepted for styrene oxide. We believe that this view must be amended for dihydronaphthalene oxide, **1**. In this system, at least, both types of pathways appear to be operating to the production of photoproducts. Our experimental and supporting computational results speak strongly that the formative events of the reaction occur on excited state surfaces or at the points of return, via conical intersections, to the ground state surface. The initial ring opening or dissociation does not deliver the excited species to the ground state as many believe. At least in this system it appears that these initial structural changes occur on the initial excited state surface or on passage to another excited state surface. Passage to a triplet surface by some of the molecules must occur early in the excited state as quenching precludes formation of **4** without increasing the yield of **2** or **3**. Irradiation at 254 nm may excite **1** (Scheme 5) to a higher singlet state surface ( $S_2$  or  $S_3$ ) from which it may pass to the  $T_1$  surface or pass to the  $S_1$  surface, possibly via C–O bond cleavage, where it could pass through distinct singlet conical intersections (HACI and AACI's), leading to the formation of **2** and **3**.

Superficially, the singlet component of this proposed mechanism is very similar to Griffin's original mechanism,<sup>5</sup> except that the "migrations" result from relaxation of the molecular geometry corresponding to conical intersection transitions to the ground state surface. Preliminary computational results support the advent of a hydrogen–allyl-type conical intersection as the mechanistic pathway for the 1,2-hydrogen migrations ubiquitously observed in these systems. Similar computational results support an alkyl–allyl-type conical intersection as the pathway for the ring contraction to form **3**, which we speculate is probably the usual pathway for 1,2-alkyl shifts in 1,3-diradical systems. The triplet pathway that we have proposed proceeds by dissociation of the oxirane moiety to a triplet arylcarbenic

### SCHEME 5. Proposed Photochemical Pathway for the Dihydronaphthalene Oxide System



aldehyde, which subsequently undergoes hydrogen abstraction by the triplet carbene, decarbonylation, then ring closure following ISC. This triplet process appears to derive from an ISC (intersystem crossing) by the excited **1** prior to significant geometric modification or very quickly after ring opening to a 1,3-diradical. Since quenching showed no signs of increased quantum yields for **2** or **3**, we speculate that the ISC occurs prior to the ring opening. Further studies into the photochemistry of this and related systems continue in our laboratories as we suspect that this type of behavior is much more ubiquitous than previously thought for aryloxiranes.

### Experimental Section

Indan (**4**), 2-tetralone (**2**), and indene (**5**) were commercially available and used as received. 1,2-Dihydronaphthalene oxide (**1**) was prepared via epoxidation of 1,2-dihydronaphthalene as described earlier,<sup>6</sup> and indane-1-carbaldehyde was prepared by a published procedure.<sup>18</sup>

Photolyses were carried out using a Rayonet photochemical reactor using 8 RPR 2537 lamps and a carousel apparatus. Direct irradiations were carried out using  $6 \times 10^{-2}$  M samples of the epoxide in quartz tubes, capped with a septum, and purged with argon for 10 min prior to irradiation. Products were analyzed with HPLC on a C-18 column using 60:40 acetonitrile/water as the solvent and a 0.75 mL/min flow rate. MS data were obtained using a ion-trap GC/MS with a temperature ramp from 50 to 250 °C using a ramp set at 8 °C/min.

Quenching studies were performed on solutions of 1,2-dihydronaphthalene oxide in acetonitrile (0.02 M) containing isoprene (0.02–1.0 M). The amount of indan formed was determined using HPLC and with toluene as an internal standard.

**Acknowledgment.** We thank the Robert A. Welch Foundation for support of this study. The support of the Gibbs–Farrington Research Chair in Chemistry (SHSU) and a Faculty Research Grant from the SHSU Research Council is also acknowledged and our gratitude expressed.

**Supporting Information Available:** Optimized atomic coordinates and energies for the computed conical intersections (CCCI, TSC, HACI, AACI1, and AACI2) and structures **7**, **TS1**, **8**, **TS2**, and **9&CO**. This material is available free of charge via the Internet at <http://pubs.acs.org>.

JO0614184

(18) Kavadias, G.; Velkof, S. *Can. J. Chem.* **1978**, *56*, 730.